Since January 2020 Elsevier has created a COVID-19 resource centre with free information in English and Mandarin on the novel coronavirus COVID-19. The COVID-19 resource centre is hosted on Elsevier Connect, the company's public news and information website.

Available online at www.sciencedirect.com
SCIENCE DIRECT
Virology 350 (2006) 15–25
VIROLOGY
www.elsevier.com/locate/yviro

Identification of critical determinants on ACE2 for SARS-CoV entry and development of a potent entry inhibitor

Dong P. Han [a], Adam Penn-Nicholson [a], Michael W. Cho [a,b,c,*]

[a] Department of Medicine, Case Western Reserve University School of Medicine, Cleveland, OH 44106, USA
[b] Department of Biochemistry, Case Western Reserve University School of Medicine, Cleveland, OH 44106, USA
[c] Department of Molecular Biology and Microbiology, Case Western Reserve University School of Medicine, Cleveland, OH 44106, USA

Received 23 November 2005; accepted 14 January 2006
Available online 28 February 2006

Abstract

Severe acute respiratory syndrome (SARS) is caused by a novel coronavirus, SARS-CoV. Virus entry into cells is mediated through interactions between spike (S) glycoprotein and angiotensin-converting enzyme 2 (ACE2). Alanine scanning mutagenesis analysis was performed to identify determinants on ACE2 critical for SARS-CoV infection. Results indicated that charged amino acids between residues 22 and 57 were important, K26 and D30, in particular. Peptides representing various regions of ACE2 critical for virus infection were chemically synthesized and evaluated for antiviral activity. Two peptides (a.a. 22–44 and 22–57) exhibited a modest antiviral activity with IC_{50} of about 50 μM and 6 μM, respectively. One peptide comprised of two discontinuous segments of ACE2 (a.a. 22–44 and 351–357) artificially linked together by glycine, exhibited a potent antiviral activity with IC_{50} of about 0.1 μM. This novel peptide is a promising candidate as a therapeutic agent against this deadly emerging pathogen.

Keywords: SARS-CoV; Pseudovirus; ACE2; Peptide; Entry inhibitor

Introduction

Severe acute respiratory syndrome (SARS) is a newly emerged disease caused by a novel coronavirus designated as SARS-CoV (Drosten et al., 2003; Ksiazek et al., 2003; Peiris et al., 2003; Poutanen et al., 2003). During the 2002–2003 epidemic, close to 8100 people were infected worldwide, among which 774 people died (WHO, 2003). Although the epidemic was relatively small in scale, the virus had a major socioeconomic impact and created global health concerns. Since then, only a few isolated incidences of SARS infection have been reported, most of which were linked to accidental exposures to the virus in a laboratory setting. However, considering the fact that some animal reservoirs that harbor the virus come into close contact with humans (Guan et al., 2003; Lau et al., 2005; Martina et al., 2003), the virus is highly likely to resurface again. Development of a vaccine and/or antiviral agents is critical to prevent future epidemics.

The entry of SARS-CoV into cells is mediated by spike (S) glycoprotein, which makes it an attractive target for development of vaccines and antiviral agents (i.e. entry inhibitors). S proteins of many coronaviruses are cleaved into, and function as, two separate subunits, S1 and S2 (Abraham et al., 1990; Jackwood et al., 2001; Mounir and Talbot, 1993); the S1 subunit binds a receptor and the S2 subunit induces fusion between viral and cellular membranes. However, S protein of SARS-CoV does not appear to be cleaved (Han et al., 2004; Xiao et al., 2003). Nevertheless, it is presumed to have two functional domains, and the border between them has been suggested to be around amino acid 680 (Lio and Goldman, 2004).

The cellular receptor for SARS-CoV has been identified as angiotensin-converting enzyme-related carboxypeptidase (ACE2) (Li et al., 2003). ACE2 is a type I integral membrane protein of 805 amino acids that contains one HEXXH + E zinc-binding consensus sequence (Donoghue et al., 2000; Tipnis et

* Corresponding author. Department of Medicine, Division of Infectious Diseases, Case Western Reserve University School of Medicine, 10900 Euclid Avenue, Cleveland, OH 44106-4984, USA. Fax: +1 216 368 0069.
E-mail address: mcho@case.edu (M.W. Cho).

0042-6822/$ - see front matter © 2006 Elsevier Inc. All rights reserved.
doi:10.1016/j.virol.2006.01.029

al., 2000). It is a homolog of angiotensin-converting enzyme (ACE), which plays an important role in the renin–angiotensin system for blood pressure homeostasis. ACE does not function as a receptor for SARS-CoV despite over 40% amino acid identity and 60% similarity to ACE2 (Li et al., 2003). It has been reported that DC-SIGNR (a protein related to DC-SIGN [dendritic cell-specific intercellular adhesion molecule-grabbing nonintegrin]) could serve as an alternative receptor (Jeffers et al., 2004). This finding, however, is contradictory to results from another study, which suggested that DC-SIGNR, as well as DC-SIGN, enhance infections mediated by ACE2 but do not function as receptors by themselves (Marzi et al., 2004). The precise role of DC-SIGN and DC-SIGNR in SARS-CoV infection and pathogenesis is yet to be elucidated.

The details of molecular interactions between SARS-CoV S protein and ACE2 are beginning to be understood. A crystal structure of ACE2 has been resolved (Towler et al., 2004), which is facilitating SARS research. A minimal receptor-binding domain (RBD) has been narrowed down to a 193 amino acid fragment (residues 318–510), which actually binds ACE2 with greater affinity than does a larger protein fragment representing the S1 domain (residues 12–672; Wong et al., 2004). Recent site-directed mutagenesis analyses of ACE2 revealed several amino acid residues important for binding S glycoprotein (Li et al., 2005b). To characterize interactions between S protein and the receptor in greater detail, we performed alanine scanning mutagenesis analyses of ACE2. The results revealed that charged amino acids between residues 22 and 57 are important for virus infection. We have applied this information in designing peptide-based entry inhibitors and identified one that has potent antiviral activity. The results of our study contribute to better understanding of SARS-CoV entry and discovery of a novel antiviral agent against the virus.

Results

Determination of amino acid residues on ACE2 critical for SARS-CoV infection

Three general regions on ACE2 have been identified to be important for binding S glycoprotein: (1) residues K31 and Y41 on α-helix 1; (2) M82, Y83 and P84 on loop 2; and (3) K353, D355 and R357 on β-sheet 5 (Li et al., 2005b). These amino acids are shown in Figs. 1B and C. To evaluate determinants of interaction between ACE2 and S glycoprotein in greater detail, we performed alanine scanning mutagenesis analyses. We focused on charged amino acid residues on α-helices 1 and 2 for two reasons. First, alignment of amino acid sequences of ACE2 and ACE, which does not support SARS-CoV infection, revealed significant divergence in these helices (only 32% and 24% identity between a.a. 20–79 of ACE2 and two homologous domains a.a. 41–100 and a.a. 644–703 of ACE, respectively; Fig. 1A). Second, electrostatic attraction is the predominant force in protein–protein interactions. Observations that residues D454 and, to a lesser degree, E452 on S glycoprotein are important for binding ACE2 (Wong et al., 2004) suggested possible interactions with oppositely charged amino acids on ACE2. We were particularly interested in the role of eight charged residues (other than K31) on α-helix 1 (residues E22, E23, K26, D30, H34, E35, E37 and D38) because they are situated near an imaginary line along amino acids already known to be important for binding S protein (Fig. 1C).

There are a total of 15 charged amino acid residues in α-helices 1 and 2 (Figs. 1A and C). We successfully mutagenized all into alanine except for D67. Mutations were introduced into a plasmid encoding a full-length ACE2 gene (Li et al., 2003). HeLa cells, which are not susceptible to SARS-CoV infection, were transfected with plasmids that encode either the wild type or mutant ACE2 proteins. These cells were infected with non-replicating SARS pseudoviruses (MuLV pseudotyped with S glycoprotein; Han et al., 2004) to determine effects of mutations on viral entry. Disappointingly, mutations had only modest effects on pseudovirus infectivity (Fig. 2A). Moreover, we were surprised to observe only about 40% reduction in infectivity for K31A mutant since Li et al. (2005b) showed near complete loss of binding activity between ACE2 and S1 protein fragment containing K31D mutation. This discrepancy could be due to the difference between pseudovirus infection and protein–protein binding assays. Alternatively, the difference could be due to the use of less drastic mutation in our study (i.e. K to A rather than K to D). Yet, another possibility was that 1-h virus adsorption period, which we routinely used, might be too long to observe subtle differences between the wild type and the mutant proteins.

To explore whether there is a difference between the wild type and mutant ACE2 in virus entry kinetics, pseudoviruses were adsorbed to cells for various times between 5 and 120 min. The kinetic analysis was performed for the wild type and D30A mutant ACE2 proteins (Fig. 2B). For the wild type ACE2, there was rapid adsorption of SARS pseudoviruses to cells between 10 and 20 min as indicated by an exponential increase in virus titer. The virus titer continued to increase up to 90 min, albeit at a slower rate. 50% maximal infection was achieved by

Fig. 1. Structure of ACE2. (A) Sequence alignment of human ACE2 and two homologous domains of human ACE. Charged amino acids are indicated in red or blue (negative and positive, respectively). K31 and Y41 are highlighted in yellow. (B) A crystal structure of ACE2 without the collectrin domain at the C-terminal end. Locations of amino acids shown to be important for binding S glycoprotein are indicated (Li et al., 2005b). α-Helices 1 and 2 are highlighted in yellow. Amino acid D615 at the C-terminus is shown as a reference. (C) Close-up view of α-helices 1 and 2. Charged amino acids are shown in red and blue. Polar and hydrophobic residues are shown in green and white, respectively. White dashed line represents an imaginary line connecting residues known to be important for binding S protein.

Fig. 4. Inhibitory effects of ACE2-derived peptides on SARS pseudovirus infection. (A) A crystal structure of an ACE2 peptide fragment (residues 22–57) as it appears in an intact protein. Five peptides derived from this fragment are shown (P1–P5). Amino acid residues are color-coded as in Fig. 1. (B) A crystal structure of ACE2 peptide fragments (residues 22–44 and 351–357). The primary sequence of peptide P6 is shown. Backbone tracing of a potential conformation of the two fragments connected by glycine is shown in the inset. (C) Inhibition of SARS pseudovirus infection as a function of concentration of six different peptides derived from ACE2. HeLa cells transfected with a plasmid expressing the wild type ACE2 were used. (D) VSV-G pseudovirus infection was not inhibited even at 100 μM.

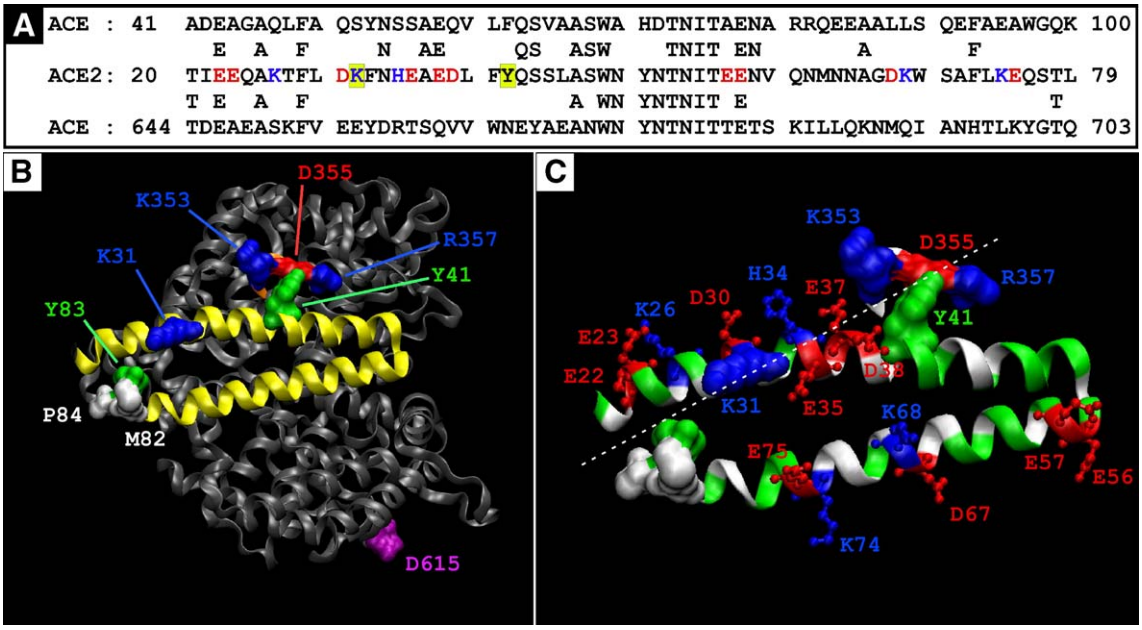
A
ACE : 41 ADEAGAQLFA QSYNSSAEQV LFQSVAASWA HDTNITAENA RRQEEAALLS QEFAEAWGQK 100
E A F N AE QS ASW TNIT EN A F
ACE2: 20 TIEEQAKTFL DKFNHEAEDL FYQSSLASWN YNTNITEENV QNMNNAGDKW SAFLKEQSTL 79
T E A F A WN YNTNIT E T
ACE : 644 TDEAEASKFV EEYDRTSQVV WNEYAEANWN YNTNITTETS KILLQKNMQI ANHTLKYGTQ 703
B
D355
K353
R357
K31
Y41
Y83
P84
M82
D615
C
K353
D355
R357
H34
E37
D30
K26
Y41
E23
E22
D38
K31
E35
K68
E75
E57
E56
D67
K74

Fig. 1.

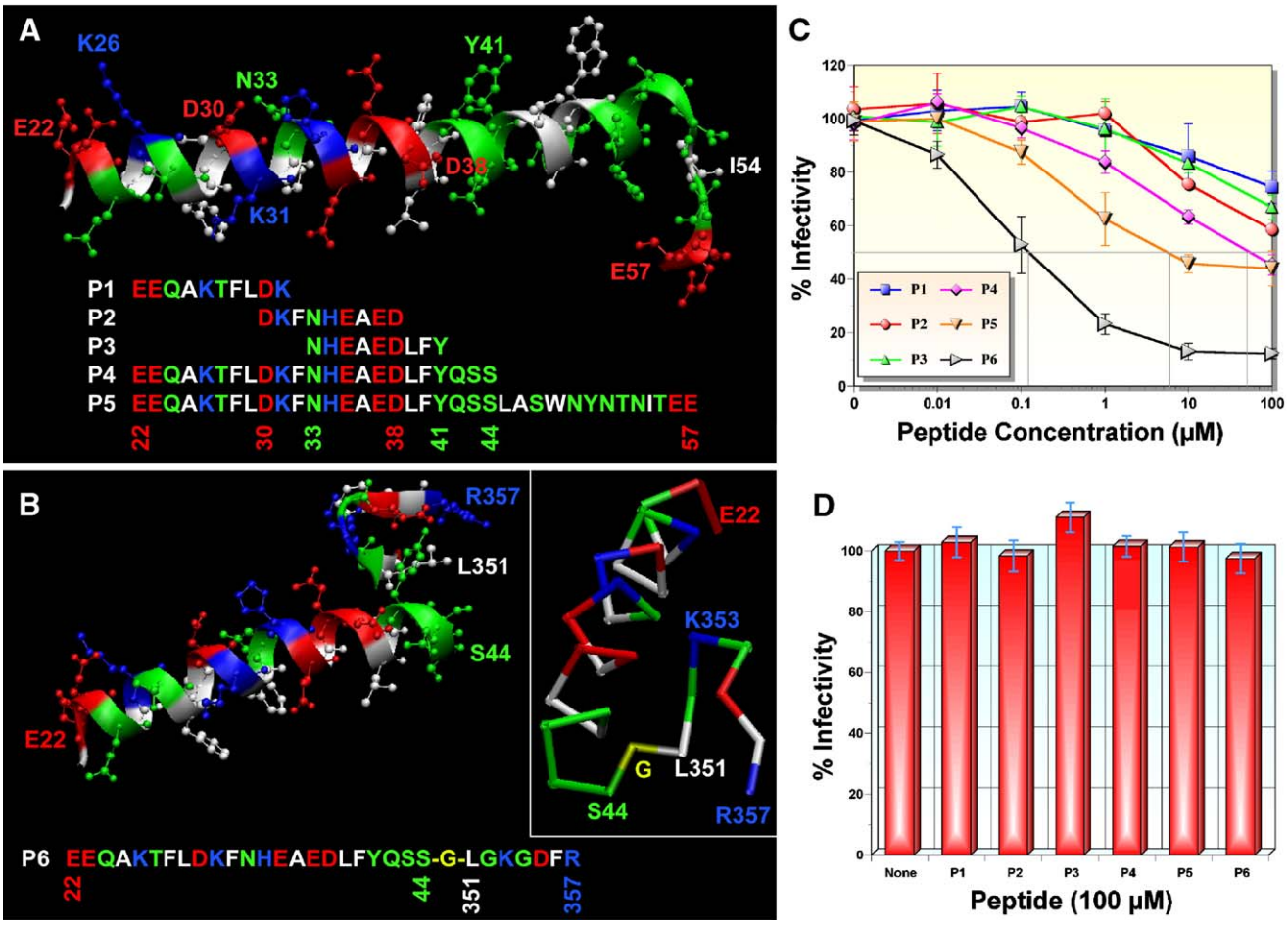
A
K26
Y41
N33
D30
E22
D38
I54
K31
E57
P1 EEQAKTFLDK
P2 DKFNHEAED
P3 NHEAEDLFY
P4 EEQAKTFLDKFNHEAEDLFYQSS
P5 EEQAKTFLDKFNHEAEDLFYQSSLASWNYNTNITEE
22 30 33 38 41 44 57
B
R357
L351
S44
E22
K353
G
L351
S44
R357
P6 EEQAKTFLDKFNHEAEDLFYQSS-G-LGKGDFR
22 44 351 357
C
% Infectivity
Peptide Concentration (μM)
P1
P2
P3
P4
P5
P6
D
% Infectivity
Peptide (100 μM)
None
P1
P2
P3
P4
P5
P6

Fig. 4.

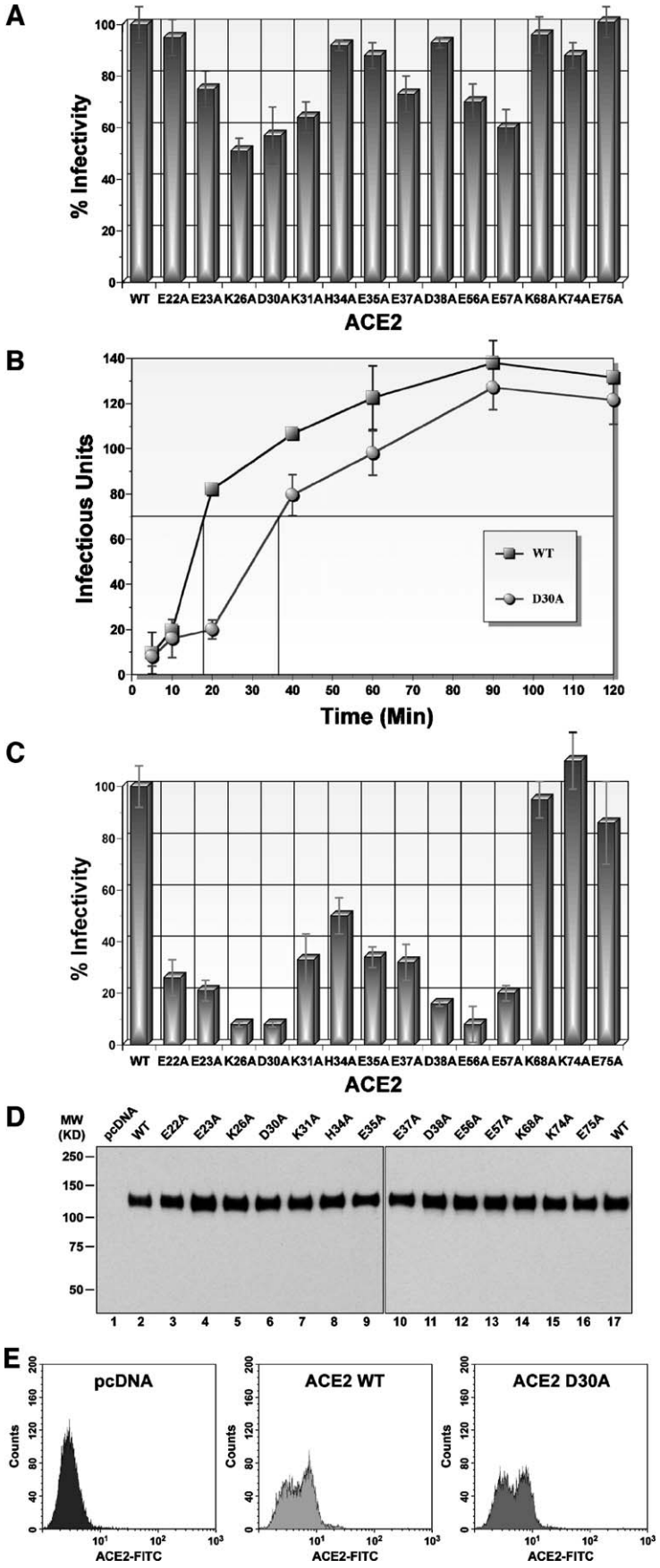
A
% Infectivity
WT E22A E23A K26A D30A K31A H34A E35A E37A D38A E56A E57A K68A K74A E75A
ACE2
B
Infectious Units
WT
D30A
Time (Min)
C
% Infectivity
WT E22A E23A K26A D30A K31A H34A E35A E37A D38A E56A E57A K68A K74A E75A
ACE2
D
MW (KD)
pcDNA WT E22A E23A K26A D30A K31A H34A E35A E37A D38A E56A E57A K68A K74A E75A WT
250
150
100
75
50
1 2 3 4 5 6 7 8 9 10 11 12 13 14 15 16 17
E
pcDNA
ACE2 WT
ACE2 D30A
Counts
ACE2-FITC

approximately 18 min. In contrast, an infection mediated by D30A mutant ACE2 was significantly slower; it took twice as long to achieve 50% maximal infection (about 36 min). More importantly, the difference in pseudovirus infectivity between the wild type and D30A ACE2 proteins was more pronounced for 20-min adsorption period compared to 60 min; very little difference was observed for adsorption periods longer than 60 min. These results suggested that different ACE2 proteins should be compared at 20 min rather than at 60 min when infectivity begins to reach a plateau. Therefore, the entire panel of ACE2 mutants was compared using a 20-min adsorption period. Under this condition, all of the mutants, except for K68A, K74A and E75A, exhibited marked reduction in their ability to support pseudovirus infection (Fig. 2C). The reduction in infectivity was not due to a defect in protein expression since all of the mutant ACE2 proteins were expressed at levels similar to that of WT ACE2 (Fig. 2D). Flow cytometry analyses of cells transfected with either WT or D30A mutant ACE2 proteins indicated that both proteins are equally expressed on the cell surface (Fig. 2E). Together, these results indicated the importance of charged amino acids between residues 22 and 57.

Effects of ACE2 concentration on the rate of pseudovirus infection

Another parameter that could potentially affect infectivity of SARS pseudoviruses is the receptor concentration. Depending on the mutation, the amount of ACE2 protein required for efficient infection could be different. Similar to how mutant ACE2 proteins required longer adsorption period, greater amounts of mutant proteins might be necessary compared to the wild type. To test this hypothesis, infectivity of SARS pseudoviruses in HeLa cells transfected with varying amounts of plasmids encoding either the wild type or D30A mutant ACE2 proteins was determined. For this experiment, 1-h adsorption period was used. As expected, SARS pseudovirus infectivity was dependent on the amount of plasmids used for both the wild type and D30A mutant ACE2 (Fig. 3A). However, greater amount of DNA was needed for D30A mutant than the wild type to achieve similar infectivity; the half maximal infectivity points for the wild type and the D30A mutant were approximately 0.16 μg and 0.41 μg, respectively. To confirm that expression of ACE2 was proportional to the amount of plasmid DNA transfected, a Western immunoblot was performed. As shown in Fig. 3B, ACE2 expression correlated with the amount of DNA transfected. Expression levels of the wild type and D30A mutant proteins were comparable, suggesting that diminished infectivity with D30A mutant is likely due to reduced affinity to S protein. An immunoreactive band of an approximately 50 kDa protein was also detected in this over-exposed blot. Although the exact nature of the protein is unknown, it most likely is a cleavage product of ACE2 since the band intensity correlated with that of the authentic ACE2.

Since the difference in infectivity between the wild type and D30A mutant ACE2 was the greatest when 0.25 μg of plasmid DNA was used, the entire panel of ACE2 mutants was evaluated using 0.25 μg. Pseudovirus infectivity was assessed using two different adsorption periods (40 and 60 min). When 60-min adsorption period was used, significant reduction in infectivity was observed only for K26A and D30A mutants (Fig. 3C). Using 40-min adsorption, infectivity was markedly reduced not only for K26A and D30A mutants, but also for E56A and E57A (Fig. 3D). Together, these results suggested that K26 and D30 might be most critical for interaction with S glycoprotein. The overall infectivity pattern was very similar to 20-min adsorption period using 1 μg of plasmid DNA (Fig. 3D compared to Fig. 2C). Consistent with results from adsorption kinetics analyses (Fig. 2), ACE2 mutants K68A, K74A and E75A exhibited no defect in supporting SARS pseudovirus infections.

Inhibition of SARS-CoV infection using an ACE2-derived peptide

Knowing that charged amino acids between residues 22 and 57 of ACE2 were important for SARS-CoV entry, we next examined whether we could design peptide-based virus entry inhibitors. We rationalized that ACE2-derived peptides that bind S glycoprotein with high affinity should be able to block ACE2-S protein interaction and inhibit virus infection. Five peptides were chemically synthesized: a.a. 22–31, 30–38, 33–41, 22–44 and 22–57 (peptides P1 through P5, respectively; Fig. 4A). To assess antiviral activity, pseudoviruses were preincubated with varying concentrations of each peptide for 20 min and then allowed to infect HeLa cells expressing ACE2. As shown in Fig. 4C, shorter peptides (P1, P2 and P3) exhibited only weak antiviral activity. Longer peptides P4 and P5 were more active with approximately 50% inhibitory concentrations (IC_{50}) of 50 μM and 6 μM, respectively.

To improve antiviral activity, we considered other possibilities of incorporating residues 82–84 or 353–357 since they were also shown to be important for binding S protein (Li et al., 2005b). Upon close examination of the ACE2 crystal structure, we noticed that the spacing between S44 and L351 was sufficiently narrow enough to be filled by a single amino acid (Fig. 4B). However, the directionality of the E22–S44 fragment was opposite from that of the L351–K353 fragment. Glycine, which has the smallest side chain, has high propensity to form reverse turns. Thus, an artificial peptide of 31 amino acids was synthesized by joining fragments 22–44 and 351–357 with glycine (peptide P6; Fig. 4B). To our surprise, peptide P6

Fig. 2. Characterization of mutant ACE2 proteins. (A) Infectivity analyses of the wild type and mutant ACE2 (60-min adsorption). (B) Kinetic analyses of SARS pseudovirus entry using the wild type or D30A mutant ACE2. Pseudoviruses were adsorbed to cells for various times as indicated. (C) Infectivity analyses of the wild type and mutant ACE2 (20-min adsorption). (D) Western blot analyses of ACE2 protein expression. (E) Comparison of cell surface expression of the wild type and D30A mutant ACE2 by flow cytometry. Cells transfected with pcDNA were used as a negative control.

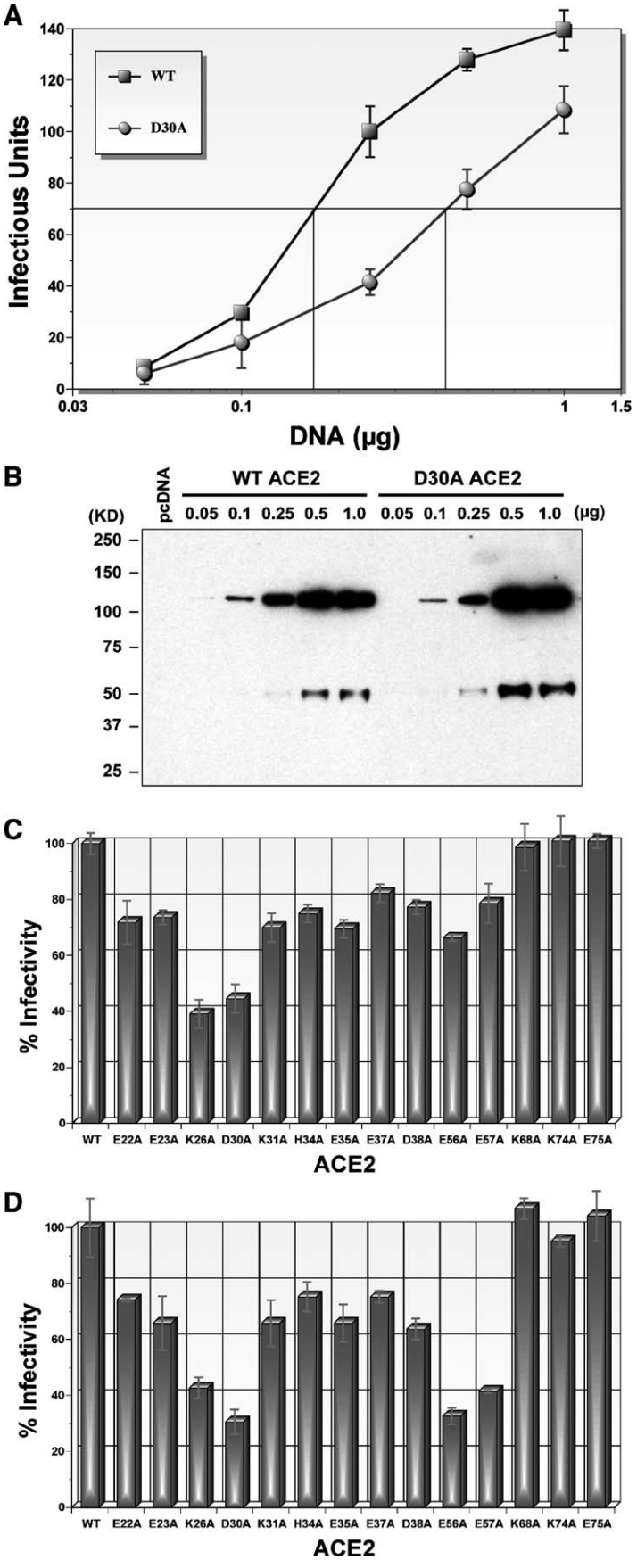
A
Infectious Units
WT
D30A
DNA (μg)
B
pcDNA
WT ACE2
D30A ACE2
(KD)
0.05 0.1 0.25 0.5 1.0 0.05 0.1 0.25 0.5 1.0 (μg)
250
150
100
75
50
37
25
C
% Infectivity
WT E22A E23A K26A D30A K31A H34A E35A E37A D38A E56A E57A K68A K74A E75A
ACE2
D
% Infectivity
WT E22A E23A K26A D30A K31A H34A E35A E37A D38A E56A E57A K68A K74A E75A
ACE2

potently inhibited SARS pseudovirus infection with an IC_{50} of approximately 0.1 μM, which is 60- and 500-fold lower than peptides P5 and P4, respectively (Fig. 5C). This was somewhat unexpected since P6 is different from P4 only by eight amino acids. Slightly higher IC_{50} value (0.3 μM) was observed when pseudovirus infections were carried out using VeroE6 cells (data not shown). The inhibitory effect is specific against SARS-CoV since none of the peptides inhibited VSV-G-pseudotyped MuLV even at 100 μM (Fig. 4D). The specificity is further evidenced by the fact that none of the peptides was effective against viruses pseudotyped with MuLV envelope protein (data not shown). No cytotoxicity was observed for peptides P4, P5 or P6 even at 200 μM based on neutral red uptake assay (data not shown).

Discussion

In this study, we examined the importance of charged amino acids in the first two α-helices of ACE2 in mediating SARS-CoV infection. Out of the total 14 residues evaluated, eleven amino acids between the residues 22 and 57 were important (E22, E23, K26, D30, K31, H34, E35, E37, D38, E56 and E57). The two most critical residues were K26 and D30. This result and the fact that all 9 charged residues between E22 and D38 played an important role were not unexpected given that they are situated in close proximity to the imaginary line that connects amino acids previously shown to be important for binding S protein fragments (Li et al., 2005b; Fig. 1C). In this regard, we were a bit surprised to see the importance of residues E56 and E57, but not K68, K74 or E75. None of the amino acids we identified was critical enough to inhibit virus infection completely. Mutants were merely less efficient than the wild type ACE2; they required either longer adsorption period or greater amounts to achieve the wild type level of infectivity. This is to be expected since there are multiple determinants of interaction between S protein and ACE2.

During the preparation of our manuscript, a crystal structure of ACE2 bound to an S protein fragment containing the RBD (residues 306 to 527) was published (Li et al., 2005a; Fig. 5A). ACE2 residues that made direct contact with the RBD included Q24, T27, K31, H34, E37, D38, Y41, Q42, L45, L79, M82, Y83, N90, Q325, E329, N330, K353 and G354. Although the crystal structure confirmed our results regarding the importance of K31, H34, E37 and D38, the study's findings did not include many of the residues we found to be important, including E22, E23, K26, D30, E35, E56 and E57 (Figs. 5B and C). We are particularly puzzled at the fact that neither K26 nor D30, the two residues that appeared to be most critical in our study, made contacts with the RBD.

There are a few possible reasons that could account for the apparent discrepancy. The simplest explanation is that results from the two studies were obtained using different S proteins. The structural study was based on a small fragment of S protein containing just the RBD. In contrast, our study was based on an intact protein. It is possible that residues other than the ones in the RBD could be making contacts with amino acids we identified.

Another possible explanation is that the conformation of the receptor-binding motif (RBM, residues 424 to 494) in the crystal structure could be somewhat different from the one in an intact S glycoprotein. It was previously shown that a D454A mutation on S protein completely abolished association of ACE2 with either the RBD (residues 318–510) or the S1 protein fragment (residues 12–672; Wong et al., 2004). Based on this result, we suspected that D454 residue might be directly interacting with ACE2. However, D454 was quite distant from ACE2 in the crystal structure (Fig. 5C). This seemingly contradictory result raises a possibility that the RBD used to solve the crystal structure may have different conformation than the one used to analyze D454A mutation; they are different in length and were prepared from different cellular sources (Sf9 insect cells vs. 293T human cells, respectively). Although it is possible that D454 plays an indirect role in binding ACE2 (e.g. in maintaining a proper conformation of the RBM), it is a little difficult to appreciate such a drastic effect from an amino acid far away from the receptor-contacting site, especially when the residue is located in a loop. A crystal structure of a larger S1 fragment is needed to resolve this issue.

A third possible reason for the discrepancy could be the difference in the nature of the two studies. The footprint analysis based on a crystal structure identifies only the residues that are making initial contacts with the RBD. In contrast, our study examined the entire virus entry process and identifies residues that are functionally important, either directly or indirectly. Therefore, the residues we identified could be involved not just in the initial binding of S glycoprotein, but in subsequent steps in the membrane fusion process. Events that follow binding of S glycoprotein to ACE2 are unknown. Additional studies are necessary to better understand the molecular details of SARS-CoV entry.

In this study, we examined anti-SARS activity of six chemically synthesized peptides derived from ACE2. The peptide with the most potent antiviral activity was P6, which is comprised of two discontinuous fragments 22–44 and 351–357 connected by glycine. Peptide P6 is just eight amino acids longer than P4. Yet, it was about 500-fold more effective. In contrast, P5, which is 13 amino acids longer than P4, was only about 8-fold more effective. It is not clear as to exactly why P6 is so much more potent than P4 or P5 peptides. The simplest explanation is that there are more residues on P6 that interact with S glycoprotein than either P4 or P5 peptides. Site-directed mutagenesis analyses indicated

Fig. 3. Characterization of mutant ACE2 proteins. (A) Analyses of SARS pseudovirus infectivity as a function of ACE2 amount. HeLa cells were transfected with indicated amounts of plasmids encoding either wild type or D30A mutant ACE2. The total amount of DNA transfected remained constant (1 μg) using pcDNA as filler DNA. (B) Western blot analyses of ACE2 expression in cells transfected with indicated amounts of plasmids expressing either wild type or D30A mutant proteins. (C) Infectivity analyses of the wild type and mutant ACE2 (0.25 μg plasmid, 60-min adsorption). (D) Infectivity analyses of the wild type and mutant ACE2 (0.25 μg plasmid, 40-min adsorption).

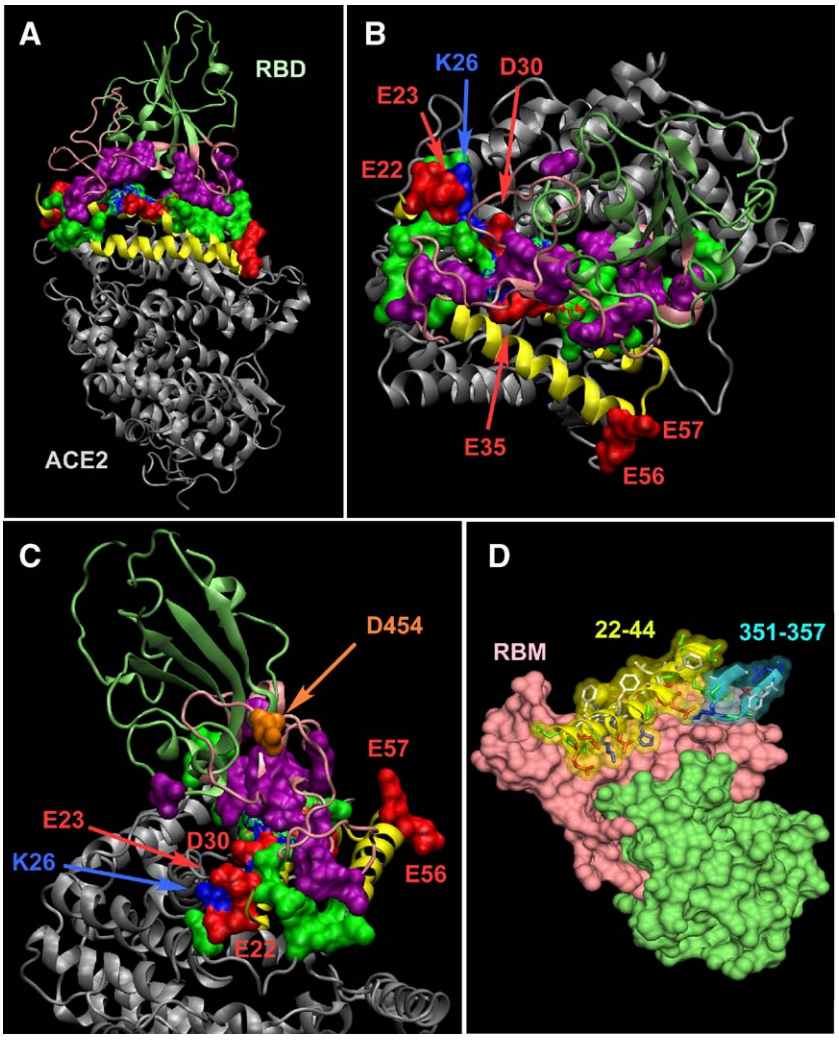

Fig. 5. Structural analyses of interactions between ACE2 and RBD. (A) A bird's eye view of a crystal structure of the RBD of S protein (lime) bound to ACE2 (gray) (Li et al., 2005a). The RBM portion of the RBD is colored pink. The surface of amino acids that actually make contacts with ACE2 is shown in purple. The first two α-helices of ACE2 are shown in yellow as a reference. ACE2 residues that make contacts with RBM are shown in green. Charged residues shown to be important for pseudovirus infection in this study are shown in either red or blue. (B) A top view of the co-crystal structure. Residues shown to be important for infection but have not shown to make contacts with the RBD are indicated. (C) A side view of the co-crystal structure. The position of D454 residue of S protein is shown in orange. (D) A potential binding site of the P6 peptide on the RBD. Peptide fragments 22–44 and 351–357 are shown in yellow and cyan, respectively. The RBM is shown in pink, while the rest of the RBD is shown in lime.

that amino acids K353, D355 and R357 are important for binding a S1 protein fragment (Li et al., 2005b). Furthermore, residues K353 and G354 make direct contacts with the RBM of S protein as shown in the crystal structure (Li et al., 2005a). Thus, four of seven residues between 351 and 357 play a role in virus infection. In contrast, only 3 of 13 amino acids between residues 45 and 57 are known to be involved in binding or mediating SARS infection (L45, E56 and E57; Li et al., 2005a and this study). However, the qualitative aspect of the interaction could be more important than simply the number of amino acids that interact between ACE2 and S protein. An interesting question that remains to be answered is whether a peptide fragment containing just the residues 351–357 could inhibit SARS infection. Assessing antiviral activity of this peptide could provide insights as to whether there is synergy between residues 22–44 and 351–357 in the context of the P6 peptide.

At the present time, we understand neither the P6 peptide structure nor how it interacts with S glycoprotein. If the peptide folds into a structure as it appears in the crystal structure of ACE2, then the peptide should bind the RBM as illustrated in Fig. 5D; the contact sites on S protein would include residues Y436, Y440, Y442, N473, Y475, N479, Y484, T486, T487, G488 and Y491. It is possible, however, that P6 may fold slightly differently as a free peptide. For one thing, residues 22–44 form a highly amphipathic α-helix; while one side of the helix that binds S protein is highly polar with many charged amino acids, the opposite side that faces interior of ACE2 is hydrophobic (Fig. 4B). These hydrophobic amino acids would be exposed to an aqueous environment in a free peptide, which might make the α-helical structure less stable. Secondly, although residues 351–357 are a part of β-turn-β structure in an intact ACE2, they might not exist in the same conformation due to the absence of other residues that support formation of

this secondary structure. Regardless, potent antiviral activity of the P6 peptide suggests that its conformation most likely resembles the one in the ACE2 crystal structure, at least when it is bound to S protein.

It has been shown that the interaction between S glycoprotein and ACE2 plays a critical role in SARS pathogenesis (Kuba et al., 2005); binding of S protein to ACE2 leads to downregulation of the receptor, which results in deregulation of the renin–angiotensin system and eventual lung injury. Therefore, our P6 peptide is a strong therapeutic candidate that would not only inhibit SARS-CoV infection but also prevent severe and often lethal lung failure.

Materials and methods

Plasmids and site-directed mutagenesis

A plasmid encoding full-length wild type human ACE2 (hACE2) was generously provided by Dr. Michael Farzan (Li et al., 2003). Site-directed mutagenesis of hACE2 was performed using QuickChangeXL Site-Directed Mutagenesis System (Stratagene) with *PfuTurbo* DNA polymerase. Fourteen pairs of primers were used to generate mutants. Primers were 33 nucleotides long, and the nucleotide changes for each of the amino acids mutated are indicated as follows: E22: gag to gCg; E23: gaa to gCa; K26: aag to GCg; D30: gac to gCc; K31: aag to GCg; H34: cac to GCc; E35: gaa to gCa; E37: gaa to gCa; D38: gac to gCc; E56: gaa to gCa; E57: gag to gCg; K68: aaa to GCa; K74: aag to GCg; and E75: gaa to gCa. Mutations were verified by sequencing.

Cell culture and pseudovirus production

Cell lines TELCeB6 (Schnierle et al., 1997), HeLa and VeroE6 were maintained in Dulbeco's modified Eagle medium (DMEM) supplemented with 5–7% fetal bovine serum, 2 mM L-glutamine and penicillin–streptomycin antibiotics. Cells were cultured in 5% CO_2 incubators at 37 °C. Pseudoviruses, which encode β-galactosidase, were produced as we have previously described (Han et al., 2004). Briefly, TELCeB6 cells, which continuously release murine leukemia virus (MuLV) particles, were transfected with plasmids encoding S glycoprotein (pHCMV-S; Han et al., 2004) or G glycoprotein of vesicular stomatitis virus (pHCMV-G; Burns et al., 1993) using Lipofectin (Invitrogen) as per manufacturer's protocol. Three days post-transfection, cell culture medium was harvested and subjected to centrifugation (1700×g, 10 min) to remove cell debris. Supernatant was aliquoted, stored at −80 °C and used as a virus stock.

To produce pseudoviruses without repeated transfections, we generated TELCeB6 cells that stably express S glycoprotein. TELCeB6 cells were co-transfected with pHCMV-S and pcDNA3.1 (Invitrogen), which encodes a neomycin resistance gene. Transfected cells were selected in the growth medium containing Geneticin (Invitrogen; 0.4 μg/ml). Geneticin-resistant clones were isolated, expanded and those able to produce high titers of SARS pseudoviruses were selected. Although cells were subsequently maintained in the absence of Geneticin, they continuously produced pseudoviruses with titers of $5–6 \times 10^3$ per ml. Virus titer was determined in VeroE6 cells.

Pseudovirus infections

Pseudovirus infections were done in VeroE6 cells (96-well plates) or in HeLa cells (24-well plates) transfected with plasmids encoding either the wild type or mutant ACE2 proteins. Cells were transfected with 1 μg (or indicated amounts) of plasmid DNA per well using Lipofectin. After overnight incubation, culture medium was replaced. Approximately 24 h post-transfection, cells were infected with about 150 infectious units of pseudoviruses. Pseudoviruses were allowed to adsorb onto cells for various times as indicated. Cells were subsequently washed with PBS to remove unadsorbed viruses, and fresh medium was added. Infections were allowed to proceed for additional 1.5 days at which time infected cells were stained with X-Gal as previously described (Han et al., 2004). Although blue cells can be detected within a few hours, staining was routinely done overnight because it yields a stronger signal. Pseudovirus-infected cells were quantified visually using inverted microscope.

Peptide synthesis and inhibition assays

Peptides were synthesized by Fmoc strategy on an Omega 396 synthesizer (Advanced ChemTech, Louisville, KY) using solid phase chemistry. Synthesis was performed by coupling amino acid esters of 1-hydroxybenzotriazole using 1,3 diisopropylcarbodiimide. Amino- and carboxyl-termini were acetylated and amidated, respectively. Deprotection of Na-Fmoc group was accomplished by 25% piperidine in dimethylformamide. After the synthesis, peptides were cleaved from the solid support and deprotected using a modified reagent K cocktail consisting of 88% TFA, 3% thioanisole, 5% ethanedithiole, 2% water and 2% phenol. The cocktail-containing peptides were filtered on a Quick-Snap column, and the filtrate was collected in 20 ml ice-cold butane ether. Peptides were precipitated (1 h at −20 °C), centrifuged and washed twice with ice-cold methyl-*t*-butyl ether. Peptides were dissolved in 25% acetonitrile and lyophilized to complete dry powder. The expected molecular weights of peptides were verified by matrix-assisted laser desorption ionization time-of-flight (MALDI-TOF) mass spectrometry. Peptides were dissolved in PBS (0.5 to 2 mM depending on peptides) and stored at −80 °C until use.

To evaluate antiviral activity, pseudoviruses (SARS-S or VSV-G) were preincubated with indicated concentrations of peptides for 20 min at 37 °C. Subsequently, the virus–peptide mixture was added to VeroE6 cells or HeLa cells transfected with a plasmid encoding the wild type ACE2. After a 20-min adsorption period, the virus inoculum was removed and fresh culture medium was added. Following additional 1.5 days of infection, infected cells were stained and virus-infected cells were quantified as described above.

Western blot and flow cytometry analyses

HeLa cells grown in 24-well plates were transfected with indicated amounts of plasmid DNA encoding either the wild type or mutant ACE2 using Lipofectin. After overnight incubation, culture medium was replaced. At 48 h post-transfection, culture medium was removed and cells were lysed with a hypotonic buffer containing non-ionic detergent (10 mM Tris, pH 7.5, 10 mM NaCl, 1.5 mM $MgCl_2$ and 1% NP-40). Nuclei and insoluble cell debris were removed by centrifugation. Cell lysates were subjected to SDS-PAGE followed by electrotransfer to nitrocellulose membranes for Western blots. ACE2 proteins were detected with rabbit anti-ACE2 polyclonal antibodies (ΨProSci Inc.) followed by goat anti-rabbit IgG conjugated with horseradish peroxidase (Pierce). Protein bands were visualized with SuperSignal chemiluminescent substrates (Pierce) according to a manufacturer's protocol.

For flow cytometry, transfected cells were harvested by scraping them into culture medium and centrifugation. Cells were washed twice with PBS and resuspended in 50 μl of Stain Buffer (BD Pharmingen) containing 0.1 μg/ml of Mouse IgG_{2A} anti-human ACE2 ectodomain monoclonal antibody (R&D Systems, # MAB9331). After staining for 1 h at 4 °C, cells were washed three times with PBS and resuspended in 50 μl of Stain Buffer containing goat-anti mouse IgG conjugated to FITC (BD Pharmingen). After staining for 1 h at 4 °C, cells were washed three times with PBS, resuspended in 300 μl of PBS and subjected to flow cytometry analysis using BD FACSCalibur.

Acknowledgments

We would like to thank Dr. Michael Farzan for providing the hACE2 plasmid and Dr. Chitra Upadhyay for technical assistance. We also thank Dr. Satya Yadav at the Molecular Biotechnology Core laboratory of the Lerner Research Institute for peptide synthesis. This work was supported by NIH grant U54 AI057160 to the Midwest Regional Center of Excellence for Biodefense and Emerging Infectious Diseases Research (MRCE) and by NIH developmental grant R21 AI059217.

References

Abraham, S., Kienzle, T.E., Lapps, W., Brian, D.A., 1990. Deduced sequence of the bovine coronavirus spike protein and identification of the internal proteolytic cleavage site. Virology 176 (1), 296–301.

Burns, J.C., Friedmann, T., Driever, W., Burrascano, M., Yee, J.K., 1993. Vesicular stomatitis virus G glycoprotein pseudotyped retroviral vectors: concentration to very high titer and efficient gene transfer into mammalian and nonmammalian cells. Proc. Natl. Acad. Sci. U.S.A. 90 (17), 8033–8037.

Donoghue, M., Hsieh, F., Baronas, E., Godbout, K., Gosselin, M., Stagliano, N., Donovan, M., Woolf, B., Robison, K., Jeyaseelan, R., Breitbart, R.E., Acton, S., 2000. A novel angiotensin-converting enzyme-related carboxypeptidase (ACE2) converts angiotensin I to angiotensin 1–9. Circ. Res. 87 (5), E1–E9.

Drosten, C., Gunther, S., Preiser, W., van der Werf, S., Brodt, H.R., Becker, S., Rabenau, H., Panning, M., Kolesnikova, L., Fouchier, R.A., Berger, A., Burguiere, A.M., Cinatl, J., Eickmann, M., Escriou, N., Grywna, K., Kramme, S., Manuguerra, J.C., Muller, S., Rickerts, V., Sturmer, M., Vieth, S., Klenk, H.D., Osterhaus, A.D., Schmitz, H., Doerr, H.W., 2003. Identification of a novel coronavirus in patients with severe acute respiratory syndrome. N. Engl. J. Med. 348 (20), 1967–1976.

Guan, Y., Zheng, B.J., He, Y.Q., Liu, X.L., Zhuang, Z.X., Cheung, C.L., Luo, S.W., Li, P.H., Zhang, L.J., Guan, Y.J., Butt, K.M., Wong, K.L., Chan, K.W., Lim, W., Shortridge, K.F., Yuen, K.Y., Peiris, J.S., Poon, L.L., 2003. Isolation and characterization of viruses related to the SARS coronavirus from animals in southern China. Science 302 (5643), 276–278.

Han, D.P., Kim, H.G., Kim, Y.B., Poon, L.L., Cho, M.W., 2004. Development of a safe neutralization assay for SARS-CoV and characterization of S-glycoprotein. Virology 326 (1), 140–149.

Jackwood, M.W., Hilt, D.A., Callison, S.A., Lee, C.W., Plaza, H., Wade, E., 2001. Spike glycoprotein cleavage recognition site analysis of infectious bronchitis virus. Avian Dis. 45 (2), 366–372.

Jeffers, S.A., Tusell, S.M., Gillim-Ross, L., Hemmila, E.M., Achenbach, J.E., Babcock, G.J., Thomas Jr., W.D., Thackray, L.B., Young, M.D., Mason, R.J., Ambrosino, D.M., Wentworth, D.E., Demartini, J.C., Holmes, K.V., 2004. CD209L (L-SIGN) is a receptor for severe acute respiratory syndrome coronavirus. Proc. Natl. Acad. Sci. U.S.A. 101 (44), 15748–15753.

Ksiazek, T.G., Erdman, D., Goldsmith, C.S., Zaki, S.R., Peret, T., Emery, S., Tong, S., Urbani, C., Comer, J.A., Lim, W., Rollin, P.E., Dowell, S.F., Ling, A.E., Humphrey, C.D., Shieh, W.J., Guarner, J., Paddock, C.D., Rota, P., Fields, B., DeRisi, J., Yang, J.Y., Cox, N., Hughes, J.M., LeDuc, J.W., Bellini, W.J., Anderson, L.J., 2003. A novel coronavirus associated with severe acute respiratory syndrome. N. Engl. J. Med. 348 (20), 1953–1966.

Kuba, K., Imai, Y., Rao, S., Gao, H., Guo, F., Guan, B., Huan, Y., Yang, P., Zhang, Y., Deng, W., Bao, L., Zhang, B., Liu, G., Wang, Z., Chappell, M., Liu, Y., Zheng, D., Leibbrandt, A., Wada, T., Slutsky, A.S., Liu, D., Qin, C., Jiang, C., Penninger, J.M., 2005. A crucial role of angiotensin converting enzyme 2 (ACE2) in SARS coronavirus-induced lung injury. Nat. Med. 11 (8), 875–879.

Lau, S.K., Woo, P.C., Li, K.S., Huang, Y., Tsoi, H.W., Wong, B.H., Wong, S.S., Leung, S.Y., Chan, K.H., Yuen, K.Y., 2005. Severe acute respiratory syndrome coronavirus-like virus in Chinese horseshoe bats. Proc. Natl. Acad. Sci. U.S.A. 102 (39), 14040–14045.

Li, W., Moore, M.J., Vasilieva, N., Sui, J., Wong, S.K., Berne, M.A., Somasundaran, M., Sullivan, J.L., Luzuriaga, K., Greenough, T.C., Choe, H., Farzan, M., 2003. Angiotensin-converting enzyme 2 is a functional receptor for the SARS coronavirus. Nature 426 (6965), 450–454.

Li, F., Li, W., Farzan, M., Harrison, S.C., 2005a. Structure of SARS coronavirus spike receptor-binding domain complexed with receptor. Science 309 (5742), 1864–1868.

Li, W., Zhang, C., Sui, J., Kuhn, J.H., Moore, M.J., Luo, S., Wong, S.K., Huang, I.C., Xu, K., Vasilieva, N., Murakami, A., He, Y., Marasco, W.A., Guan, Y., Choe, H., Farzan, M., 2005b. Receptor and viral determinants of SARS-coronavirus adaptation to human ACE2. EMBO J. 24 (8), 1634–1643.

Lio, P., Goldman, N., 2004. Phylogenomics and bioinformatics of SARS-CoV. Trends Microbiol. 12 (3), 106–111.

Martina, B.E., Haagmans, B.L., Kuiken, T., Fouchier, R.A., Rimmelzwaan, G.F., Van Amerongen, G., Peiris, J.S., Lim, W., Osterhaus, A.D., 2003. Virology: SARS virus infection of cats and ferrets. Nature 425 (6961), 915.

Marzi, A., Gramberg, T., Simmons, G., Moller, P., Rennekamp, A.J., Krumbiegel, M., Geier, M., Eisemann, J., Turza, N., Saunier, B., Steinkasserer, A., Becker, S., Bates, P., Hofmann, H., Pohlmann, S., 2004. DC-SIGN and DC-SIGNR interact with the glycoprotein of Marburg virus and the S protein of severe acute respiratory syndrome coronavirus. J. Virol. 78 (21), 12090–12095.

Mounir, S., Talbot, P.J., 1993. Molecular characterization of the S protein gene of human coronavirus OC43. J. Gen. Virol. 74 (Pt 9), 1981–1987.

Peiris, J.S., Lai, S.T., Poon, L.L., Guan, Y., Yam, L.Y., Lim, W., Nicholls, J., Yee, W.K., Yan, W.W., Cheung, M.T., Cheng, V.C., Chan, K.H., Tsang, D.N., Yung, R.W., Ng, T.K., Yuen, K.Y., 2003. Coronavirus as a possible cause of severe acute respiratory syndrome. Lancet 361 (9366), 1319–1325.

Poutanen, S.M., Low, D.E., Henry, B., Finkelstein, S., Rose, D., Green, K., Tellier, R., Draker, R., Adachi, D., Ayers, M., Chan, A.K., Skowronski, D. M., Salit, I., Simor, A.E., Slutsky, A.S., Doyle, P.W., Krajden, M., Petric, M., Brunham, R.C., McGeer, A.J., 2003. Identification of severe acute respiratory syndrome in Canada. N. Engl. J. Med. 348 (20), 1995–2005.

Schnierle, B.S.S., J., Bosch, V., Nocken, F., Merget-Millitzer, H., Engelstadter, M., Kurth, R., Groner, B., Cichutek, K., 1997. Pseudotyping of murine leukemia virus with the envelope glycoproteins of HIV generates a retroviral vector with specificity of infection for CD4-expressing cells. Proc. Natl. Acad. Sci. U.S.A. 94 (16), 8640–8645.

Tipnis, S.R., Hooper, N.M., Hyde, R., Karran, E., Christie, G., Turner, A.J., 2000. A human homolog of angiotensin-converting enzyme. Cloning and functional expression as a captopril-insensitive carboxypeptidase. J. Biol. Chem. 275 (43), 33238–33243.

Towler, P., Staker, B., Prasad, S.G., Menon, S., Tang, J., Parsons, T., Ryan, D., Fisher, M., Williams, D., Dales, N.A., Patane, M.A., Pantoliano, M.W., 2004. ACE2 X-ray structures reveal a large hinge-bending motion important for inhibitor binding and catalysis. J. Biol. Chem. 279 (17), 17996–18007.

WHO, 2003. Summary of probable SARS cases with onset of illness from 1 November 2002 to 31 July 2003. World Health Organization.

Wong, S.K., Li, W., Moore, M.J., Choe, H., Farzan, M., 2004. A 193-amino acid fragment of the SARS coronavirus S protein efficiently binds angiotensin-converting enzyme 2. J. Biol. Chem. 279 (5), 3197–3201.

Xiao, X., Chakraborti, S., Dimitrov, A.S., Gramatikoff, K., Dimitrov, D.S., 2003. The SARS-CoV S glycoprotein: expression and functional characterization. Biochem. Biophys. Res. Commun. 312 (4), 1159–1164.